Stereochemical Retention of the Configuration in the Action of Fhit on Phosphorus-Chiral Substrates†

Andreas Abend,‡ Preston N. Garrison,§ Larry D. Barnes,*,§ and Perry A. Frey*,‡

Institute for Enzyme Research, The Graduate School, and Department of Biochemistry, College of Agricultural and Life Sciences, University of Wisconsin−Madison, Madison, Wisconsin 53705, and Department of Biochemistry, University of Texas Health Science Center, San Antonio, Texas 78284-7760

Received August 6, 1998; Revised Manuscript Received February 5, 1999

ABSTRACT: Fhit is the protein product of *FHIT*, a candidate human tumor suppressor gene. Fhit catalyzes the hydrolysis of diadenosine triphosphate (Ap_3A) to AMP and ADP. Fhit is here shown to catalyze the hydrolysis in $H_2{}^{18}O$ with production of adenosine 5′-[^{18}O]phosphate and ADP, proving that the substitution of water is at P_α and not at P_β. The chain fold of Fhit is similar to that of galactose-1-phosphate uridylyltransferase, which functions by a double-displacement mechanism through the formation of a covalent nucleotidyl−enzyme intermediate and overall retention of configuration at P_α. The active site of Fhit contains a histidine motif that is reminiscent of the HPH motif in galactose-1-phosphate uridylyltransferases, in which the first histidine residue serves as the nucleophilic catalyst to which the nucleotidyl group is bonded covalently in the covalent intermediate. In this work, the Fhit-catalyzed cleavage of (R_P)- and (S_P)-γ-(*m*-nitrobenzyl) adenosine 5′-*O*-1-thiotriphosphate (*m*NBATPαS) in $H_2{}^{18}O$ to adenosine 5′-[^{18}O]thiophosphate is shown to proceed with overall retention of configuration at phosphorus. γ-(*m*-Nitrobenzyl) adenosine 5′-*O*-triphosphate (*m*NBATP) is approximately as good a substrate for Fhit as Ap_3A, and both (R_P)- and (S_P)-*m*NBATPαS are substrates that react at about 0.5% of the rate of Ap_3A. The stereochemical evidence indicates that hydrolysis by Fhit proceeds by a double-displacement mechanism, presumably through a covalent AMP−enzyme intermediate.

FHIT is a candidate human tumor suppressor gene that spans the FRA3B fragile site and the t(3;8) translocation breakpoint at chromosome 3pl4.2 (*1*). Homozygous deletions in the *FHIT* locus have been observed in cell lines derived from a number of different tumors, and aberrant transcripts have been observed in different types of primary tumors (*2*−*5*). Recently, Siprashvili et al. (*6*) demonstrated that stable transfection of *FHIT*$^-$ cancer cell lines with *FHIT* suppressed tumorigenicity of the cells in nude mice.

Insight into the function of the Fhit[1] protein was provided by its homology to Ap_4A asymmetrical hydrolase from the fission yeast, *Schizosaccharomyces pombe* (*1*, *7*). Fhit proved to be a dinucleoside 5′-oligophosphate hydrolase as well, although its preferred substrate is Ap_3A (EC 3.6.1.29) (*8*). Another Fhit homologue, the *Saccharomyces cerevisiae* Aphl/Hnt2 protein, has recently been shown to also be an Ap_3A hydrolase (*9*). These proteins constitute an exclusively eukaryotic branch of the HIT family of proteins. HIT proteins contain four conserved histidine residues, three of which occur in a triad, HxHxHxx, where x represents a hydrophobic residue (*10*). The other branch of the HIT family includes the Hint proteins, which occur in all branches of life (*11*). They are probably nucleotidyl transferases or hydrolases, but no good substrate has yet been reported. More distant relatives of the HIT proteins, galactose-l-phosphate uridylyltransferases (EC 2.7.7.12) (GalT) and Ap_4A phosphorylases (EC 3.6.1.17), were identified on the basis of limited sequence similarities surrounding the histidine triad region (*7*).[2] In these enzymes, glutamine replaces histidine in the third position of the triad. The conserved sequence includes

† Supported by NSF Grant MCB-9604124 (L.D.B.) and Grant GM30480 from the National Institute of General Medical Sciences (P.A.F.). A.A. was sponsored by the Deutsche Forschungsgemeinshaft. This study made use of the National Magnetic Resonance Facility at Madison, which is supported by NIH Grant RR02301 from the Biomedical Research Technology Program, National Center for Research Resources. Equipment in the facility was purchased with funds from the University of Wisconsin, the NSF Biological Instrumentation Program (Grant DMB-8415048), the NIH Biomedical Research Technology Program (Grant RR02301), the NIH Shared Instrumentation Program (Grant RR02781), and the U.S. Department of Agriculture.

‡ University of Wisconsin−Madison.

§ University of Texas Health Science Center.

[1] Abbreviations: Fhit, fragile histidine triad; HIT, histidine triad; Hint, nucleotide-binding histidine triad; PKCI, protein kinase C-interacting protein; AK, adenylate kinase; PK, pyruvate kinase; LDH, lactate dehydrogenase; AMPS, adenosine 5′-phosphorothioate; Ap_3A, diadenosine 5′-*O*-5‴-*O*-P^1,P^3-triphosphate; Ap_4A, diadenosine 5′,5‴-P^1,P^4-tetraphosphate; *m*NBDP, *m*-nitrobenzyl diphosphate; *m*NBATP, γ-(*m*-nitrobenzyl) ATP; (R_P)-*m*NBATPαS, (R_P)-γ-(*m*-nitrobenzyl) adenosine 5′-*O*-(1-thiotriphosphate); (S_P)-*m*NBATPαS, (S_P)-γ-(*m*-nitrobenzyl) adenosine 5′-*O*-(1-thiotriphosphate); ATPαS, adenosine 5′-*O*-(1-thiotriphosphate); Gp_3A, P^1-5′-*O*-guanosine P^3-5′-*O*-adenosine triphosphate; AMPS,$^{18}O_1$, adenosine 5′-thio[$^{18}O_1$]phosphate; (S_P)-ATPαS,$^{18}O_1$, (S_P)-adenosine 5′-1-thio[1-$^{18}O_1$]triphosphate; DTT, dithiothreitol; PMSF, phenylmethanesulfonyl fluoride; HEPES, *N*-(2-hydroxyethyl)piperazine-*N*′-2-ethanesulfonic acid; DEAE, diethylaminoethyl; DMF, dimethylformamide; SDS−PAGE, sodium dodecyl sulfate−polyacrylamide gel electrophoresis; TEAB, triethylammonium bicarbonate; DTT, dithiothreitol; EDTA, ethylenediaminetetraacetic acid; PP_i, inorganic pyrophosphate; FPLC, fast protein liquid chromatography; HPLC, high-performance liquid chromatography; NMR, nuclear magnetic resonance; UV/vis, ultraviolet/visible.

[2] P. N. Garrison, unpublished results.

10.1021/bi981895j CCC: $18.00
Published on Web 03/05/1999

the active site region of *Escherichia coli* GalT (*12*). The structural relationship among these proteins was confirmed upon determination of the three-dimensional structures of *E. coli* GalT (*13*), rabbit and human Hint (*11*, *14*, *15*), and human Fhit (*16*, *17*). This group of nucleotidyl transferases and hydrolases has been designated as the GAFH (**G**alT, **A**p$_4$A phosphorylase, **F**hit, and **H**int) superfamily (*5*).

The structural similarities among these enzymes, including the close correspondence of nucleotide-bound forms, suggests that they function by similar mechanisms. The catalytic mechanism of *E. coli* GalT has been characterized extensively. The enzyme catalyzes the reaction of galactose-1-phosphate with UDP-glucose in a double-displacement mechanism by way of a nucleotidylated histidine−enzyme intermediate (*18*, *19*). The reaction proceeds with overall retention of the stereochemical configuration at the α-phosphorus, a result expected for the ping-pong bi-bi kinetic mechanism of the reaction (*18*, *20*). Each of the two steps of the double displacement mechanism proceeds with inversion of configuration at P, leading to overall retention of configuration (*21*). The histidine that serves as a nucleophile and is uridylylated in the reaction is residue 166 (*12*, *22*, *23*). His166 in *E. coli* GalT corresponds to the central histidine in the histidine triad in HIT proteins in general, and specifically to His96 in Fhit.

Previous studies have indicated that His96 of Fhit is critical for activity. A His96Asn mutation had only a small effect on K_m but decreased k_{cat} 10^6-fold (*17*). Similar mutations of the other conserved histidines had much smaller effects (*8*). Evidence has also been reported for formation of a covalent nucleotidyl−enzyme intermediate in a reaction of ATP with Fhit (*24*). The nucleotidyl−enzyme intermediate was not characterized stoichiometrically or structurally or as an intermediate. It was thus of interest to determine if the reaction of Fhit would proceed with retention of configuration at P, as expected for a double-displacement mechanism. Here we report the stereochemistry of the reaction catalyzed by Fhit using diastereomers of an ATP analogue. We observed retention of configuration at the α-phosphorus in the hydrolysis of these substrates. This study extends the sequence and structural similarity among proteins of the GAFH superfamily to include mechanistic similarity.

EXPERIMENTAL PROCEDURES

Enzymes. Human Fhit was isolated from *E. coli* strain SG100 transformed with pSGA02, harboring the Fhit gene, according to the methods of Brenner et al. (*25*) with slight modifications. Bacteria (15 g) were disrupted in a French press in a total volume of 50 mL [50 mM HEPES (pH 6.8) and 10% glycerol] in the presence of 3 mM DTT, 0.5 mM PMSF, 2 mM EDTA, 5 mM benzamidine, and 5 units/mL Benzonase. The crude enzyme extract was centrifuged at 100000*g* for 30 min at 4 °C and diluted 2-fold with water/10% glycerol to 25 mM HEPES (buffer A). The enzyme solution was then loaded onto a DEAE-Fractogel column (30 cm × 2.5 cm) equilibrated in buffer A via a Superloop (150 mL, Pharmacia) on a FPLC system. After a 300 mL wash, a gradient from 0 to 50% buffer B (400 mM NaCl in buffer A, pH 6.8) in a total volume of 1200 mL (flow rate of 5 mL/min) was started. Two peaks showing Fhit activity were well-resolved and checked for purity via SDS−PAGE. The active fractions were pooled and concentrated under N_2 pressure on a Amicon YM 10 membrane to a final volume of 7.5 mL. The total activity was 100 units/mg protein. The enzyme was stored at −20 °C.

Adenylate kinase was from Boehringer Mannheim. Pyruvate kinase and lactate dehydrogenase were from Sigma. Benzonase was from E. Merck.

Chemicals. Alumina B, Super I (activated Al_2O_3, basic), was from Alltech. PMSF, EDTA-Na_2, HEPES, Ap$_3$A, adenosine, and benzamidine were from Sigma. DTT, triethylamine, and glycerol were from Fisher. Anhydrous solvents (DMF, pyridine, 1,4-dioxane, diethyl ether, methanol, and acetonitrile) as well as *m*-nitrobenzyl bromide, tetra-*n*-butylammonium hydroxide (40% in water), diphenyl phosphorochloridate, triethyl phosphate, tri-*n*-octylamine, and tri-*n*-butylamine were from Aldrich. $H_2{}^{18}O$ (99%) was from Isotec. Triethyl phosphate and tri-*n*-butylamine were dried over CaH_2, vacuum distilled, and stored at 4 °C in a desiccator. Dioxane and ether were passed over activated basic Al_2O_3 prior to use. Triethylammonium bicarbonate (TEAB, 1 M) buffer was prepared by passing CO_2 through a glass fritted tube into a solution containing 2250 mL of water and 350 mL of freshly distilled triethylamine until the pH of the solution was 7.3.

Chromatographic System. Most nucleotides and Fhit were purified using a FPLC system (Pharmacia). For nucleotides, a Superformance glass cartridge (2.5 cm × 30 cm or 2.5 cm × 15 cm, EM Science) was packed with DEAE-Sephadex A-25 (Pharmacia) under a flow rate of 10 mL/min in 1 M TEAB on the FPLC system. Anion-exchange separation of Fhit from the crude cell extract on DEAE-Fractogel (EM Science) was performed using a Superformance glass cartridge (2.5 cm × 30 cm, packed in 1 M NaCl as described for the A-25 column). Epimeres of *m*NBATPαS were separated on a preparative RP-18 column (2.2 cm × 30 cm, Econosil, 5 μm, Alltech) using a Waters HPLC system. Enzyme kinetics were determined on a Beckman HPLC system connected to an autosampler (Shimadzu) using an analytical anion-exchange column (25 cm × 4.6 cm, SAX) from Vydac.

Enzyme Kinetics. The method described by Barnes et al. (*8*) was used for rate measurements to determine the kinetic parameters for the reactions of *m*NBATP and its phosphorothioate analogues. The enzymatic reaction (in 1 mL) was quenched with 2 M $HClO_4$ on ice and the mixture brought to pH 4 with 10 N KOH. A 200 μL aliquot was injected onto the column using the autosampler. The gradient was 5% B from 0 to 2 min, 5 to 75% B from 2 to 15 min, and 75% B from 15 to 18 min (A is 50 mM Na_2HPO_4 at pH 4.1; B is 1 M NaCl in A at pH 3.8). The separation of AMP (R_f = 4.8 min), AMPS (R_f = 7 min), ADP (R_f = 7.7 min), *m*NBDP (R_f = 9 min), and the respective substrates [Ap$_3$A (R_f = 12.2 min), *m*NBATP (R_f = 13 min), and (S_P)- and (R_P)-*m*NBATPαS (R_f = 15.5 min)] was monitored at 260 nm. The peak areas under the product and substrate peaks were added and corrected for the ratio of the absorbance coefficients for the individual compounds [$\epsilon_{Ap_3A} = 24$ μmol/cm^2, $\epsilon_{mNBATP} = \epsilon_{(S_p)-mNBATP\alpha S} = \epsilon_{(R_p)-mNBATP\alpha S} = 20.66$ μmol/cm^2, $\epsilon_{AMP} = \epsilon_{ADP} = \epsilon_{AMPS} = 15$ μmol/cm^2, and $\epsilon_{mNBDP} = 5.8$ μmol/cm^2]. To calculate the percent hydrolysis of the substrate, only the area under one product peak (e.g., AMP in the case of *m*NBATP) was divided by the area of the sum of the areas of AMP and *m*NBATP. This number was then

multiplied by the amount of substrate in the reaction mixture to yield the total amount of substrate hydrolyzed per time unit (usually 10 min). These data points were plotted against the substrate concentration and fitted by the Michaelis−Menten equation.

A coupled spectrophotometric enzyme assay (*26*) for determining the concentrations of AMP and ADP simultaneously was used as a control of the kinetic parameters obtained by the HPLC assay. The method was also useful for checking active fractions from the Fhit purification. This method in combination with the analytical HPLC method was also used to obtain the extinction coefficient of *m*NBATP at 260 nm (data not shown).

^{31}P NMR. Routine ^{31}P NMR was performed on a Bruker WP200 spectrometer. Sample concentrations were 100 mM. Analysis of chemical isotope shifts in ^{18}O-labeled nucleotides was performed on a Bruker AM 500 spectrometer (observation frequency of 202.3377 MHz, sweep width of ±12135.9 kHz, and 32 768 data points). The sample concentration was >10 mM in the presence of 1 mM EDTA (pH 8.0).

UV/vis spectroscopy was performed on a Hewlett-Packard DAD spectrophotometer.

Synthesis of mNBDP. The strategy of this synthesis is described by Davisson et al. (*27*). Pyrophosphate (30 mmol, disodium salt) was passed over a AG 50W-X8 column in the $H^{(+)}$ form (5 cm × 30 cm). Fractions were checked for conductivity or pH and pooled, and tetra-*n*-butylammonium hydroxide was added to raise the pH from 1 to 7.5. The solvent was evaporated, and the remainder was dried for 2 days under high vacuum. The white tris(tetra-*n*-butylammonium) pyrophosphate (29 mmol, 97%) was then stored in a desiccator over P_2O_5. To 5 mmol of *m*-nitrobenzyl bromide in 1 mL of anhydrous acetonitrile was added 6.25 mmol of the dry pyrophosphate, and the mixture was stirred under N_2 at room temperature. After 8 h, the ^{31}P NMR spectrum showed completion of the reaction, and the solvent was removed under reduced pressure. The residue was dissolved in 100 mL of water, and the pH was adjusted to 7.8 with 1 N NaOH. The solution was loaded onto a DEAE-Sephadex A-25 column (2.5 cm × 45 cm, equilibrated in 200 mM TEAB). The column was washed with 800 mL of 200 mM TEAB, and subsequently, a 4 L gradient from 200 to 500 mM TEAB was started. *m*NBDP (4 mmol) coeluted with pyrophosphate in 0.35 M TEAB. Fractions were pooled and evaporated to dryness. The compound (2 mmol) was passed over a cation-exchange column in the pyridine form, lyophilized, and then suspended in 20 mL of anhydrous MeOH. Solution was effected upon addition of 4.8 mmol of tri-*n*-octylamine. The solvent was removed in vacuo, the residue dissolved in 10 mL of anhydrous DMF, and the solution stored in a desiccator at −20 °C: ^{31}P NMR δ −4.75 ppm (d, $J_{\alpha,\beta}$ = 22.9 Hz, P_β), −11.0 ppm (d, $J_{\alpha,\beta}$ = 22.9 Hz, P_α); optical absorption λ_{max} = 270 nm.

Synthesis of AMPS. This compound was synthesized according to the method of Murray and Atkinson (*28*), with modifications. Adenosine (5 mmol) was dried at 110 °C over P_2O_5 in vacuo for 12 h and then dissolved in 12 mL of dry triethyl phosphate by carefully heating the reaction flask under N_2. The flask was cooled on an ice/water bath, and 15 mmol of $PSCl_3$ was added. The reaction mixture was stirred for another 30 min on the ice/water bath under N_2 and then transferred into a cold room (4 °C) and stirred for another 12 h. To the white viscous solution were added 5 mL of water and 1 g of sodium acetate in the cold, and the mixture was stirred for 4 h at 4 °C. At room temperature, 5 N NaOH was added slowly over a period of 1 h to hold the pH at 8. The solution was diluted with 200 mL of 100 mM TEAB and then charged on a DEAE-Sephadex A-25 column (2.5 cm × 45 cm, equilibrated with 200 mM TEAB). After the column had been washed with 600 mL of 200 mM TEAB, a 3000 mL gradient from 200 to 400 mM TEAB was started. AMPS (4 mmol), free of thiophosphate, eluted at 300 mM TEAB. The compound was passed over a cation-exchange column in the pyridine form, lyophilized, and then suspended in 20 mL of anhydrous MeOH. Solution was effected upon addition of 4 mmol of tri-*n*-octylamine. The solvent was removed in vacuo and the residue dissolved in 10 mL of anhydrous DMF and stored in a desiccator at −20 °C: ^{31}P NMR δ 44.250 ppm.

Synthesis of (S_P)-mNBATPαS and (R_P)-mNBATPαS. The general method of Michelson (*29*) for the synthesis of nucleotide phosphoanhydrides by anion exchange was adopted in the preparation of these compounds. AMPS (1 mmol, tri-*n*-octylammonium salt) was evaporated three times from 10 mL of anhydrous DMF. The compound was dissolved in 2 mL of anhydrous dioxane that had been passed over aluminum oxide prior to use to remove contaminating peroxides, and it was activated upon addition of 1 mmol of tri-*n*-butylamine followed by 1.5 mmol of diphenyl phosphorochloridate under N_2. The reaction mixture was stirred for 2.5 h at 25 °C, and the solvent was removed in vacuo. The residue was extracted with 50 mL of peroxide free anhydrous ether in the cold. The ether layer was decanted, and then 1 mL of dioxane was added to the precipitate and evaporated along with the remaining ether in vacuo. Dry *m*NBDP (1.5 mmol, tri-*n*-butylammonium salt) dissolved in 10 mL of anhydrous pyridine was added to the activated AMPS under N_2 and the mixture stirred for 4 h. The solvent was evaporated and the sample dissolved in 100 mL of 100 mM TEAB. The pH was adjusted to 7.8, and the compound was loaded onto a DEAE-Sephadex A-25 column (2.5 cm × 30 cm, equilibrated with 200 mM TEAB). After a 300 mL wash with 200 mM TEAB, a 3000 mL gradient from 200 to 600 mM TEAB at a flow rate of 5 mL/min was started. (R_P)-*m*NBATPαS and (S_P)-*m*NBATPαS together with *m*NBDP eluted in 440 mM TEAB. The solvent was evaporated, and TEAB was removed by repeated evaporation from 10 mL portions of ethanol/water.

The epimers were separated from each other and *m*NBDP on a preparative RP-18 column. Seventy-five micromoles of the mixture was dissolved in a total volume of 1.5 mL of 10 mM potassium phosphate and loaded at a flow rate of 8 mL/min on the column (equilibrated in 10 mM potassium phosphate/7.5% MeOH). *m*NBDP emerged after 7 min, (S_P)-*m*NBATPαS after 13 min, and (R_P)-*m*NBATPαS after 25 min. The solvent was removed; the pH was adjusted to 7.8 with 5 N NaOH, and the individual epimers were freed from phosphate by rechromatography on a DEAE-Sephadex A-25 column. The TEAB buffer was evaporated, and 1 mL of water was added; the pH was adjusted to 8.0 with 1 N NaOH, and the compounds were stored at − 20 °C. The yields were 300 μmol of (R_P)-*m*NBATPαS (200 μmol, 30% yield) and (S_P)-*m*NBATPαS (100 μmol, 10% yield): ^{31}P NMR for (S_P)-*m*NBATPαS δ 44.45 ppm (d, $J_{\alpha,\beta}$ = 24.81 Hz, P_α), −10.28

ppm (d, $J_{\gamma,\beta}$ = 21.97 Hz, P_γ), −22.887 ppm (dd, P_β); ^{31}P NMR for (R_P)-*m*NBATPαS δ 44.15 ppm (d, $J_{\alpha,\beta}$ = 26.85 Hz, P_α), −10.55 ppm (d, $J_{\gamma,\beta}$ = 19.53 Hz, P_γ), −23.115 ppm (dd, P_β).

Enzymatic Hydrolysis of Ap_3A in 50% ^{18}O-Enriched Water. Fhit (20 units) were incubated with 25 μmol of Ap_3A in a total volume of 1 mL at 37 °C in 50% $H_2{}^{18}O$-enriched buffer [50 mM HEPES (pH 6.8) and 2 mM $MgCl_2$]. The progress of the reaction was monitored by analytical HPLC. After 3 h, no remaining substrate was detectable and the reaction mixture was loaded onto a DEAE-Sephadex A-25 column (2.5 cm × 15 cm, equilibrated with 100 mM TEAB) and separated by applying a 1 L gradient from 100 to 400 mM TEAB. AMP,$^{18}O_1$, as determined by ^{31}P NMR, eluted in 250 mM TEAB, and ADP eluted in 340 mM TEAB: ^{31}P NMR for AMP,$^{18}O_1$ δ 2.562 ppm; ^{31}P NMR for AMP δ 2.600 ppm; ^{31}P NMR for ADP δ −9.22 ppm (d, $J_{\alpha,\beta}$ = 22.4 Hz, P_α), −4.50 ppm (d, $J_{\alpha,\beta}$ = 22.4 Hz, P_β).

Enzymatic Hydrolysis of (R_P)-mNBATPαS in 50% and (S_P)-mNBATPαS in 40% ^{18}O-Enriched Water. Fhit [1 mL, 1200 units, in 100 mM NaCl, 25 mM HEPES (pH 6.8), and 10% glycerol] was diluted with 14 mL of 100 mM HEPES (pH 8.0) and concentrated to a final volume of 500 μL over centricons 10 (Amicon). In a total of 2 mL, 25 μmol of (R_P)-*m*NBATPαS [(S_P)-*m*NBATPαS] was hydrolyzed in 50% (40%) ^{18}O-enriched water. NaOH (5 N) was added several times in the first 1 h to protect AMPS from desulfurization. The progress of the reaction was followed by analytical HPLC, and after 3 h, all the starting material had been hydrolyzed. The reaction products were purified as described above. AMPS,$^{18}O_1$ (18 μmol) was eluted in 280 mM TEAB and *m*NBDP in 320 mM TEAB: ^{31}P NMR for AMPS,$^{18}O_1$ δ 44.212 ppm; ^{31}P NMR for AMPS δ 44.250 ppm

Enzymatic Phosphorylation of AMPS,$^{18}O_1$ to (S_P)-ATPαS,$^{18}O_1$. AMPS,$^{18}O_1$ (15 μmol) was phosphorylated as described previously (*31*) but without LDH and NADH. The progress of the reaction was monitored by analytical HPLC. The reaction approached completion after 3 h, and ATPαS,$^{18}O_1$ was separated from the starting material on a DEAE-Sephadex A-25 column (2.5 cm × 15 cm, equilibrated with 150 mM TAEB) using a 1 L gradient from 150 to 700 mM TEAB. ATPαS,$^{18}O_1$ (12 μmol) emerged in 550 mM TEAB and was freed of TEAB as described above: ^{31}P NMR (for ^{18}O-labeled compounds, see Table 1) for (S_P)-ATPαS δ 44.301 ppm (d, $J_{\alpha,\beta}$ = 22.1 Hz, P_α), −4.47 ppm (d, $J_{\gamma,\beta}$ = 22.7 Hz, P_γ), −22.301 ppm (dd, P_β).

RESULTS AND DISCUSSION

Orientation of Fhit-Catalyzed Hydrolysis in Triphosphates. To determine the stereochemical consequence of Fhit-catalyzed hydrolysis of Ap_3A by the use of phosphorothioates, we had to determine which phosphorus atom is the target of the nucleophilic attack by water which produces AMP and ADP regardless of the kinetic mechanism involved (Figure 1). Carrying out the enzymatic reaction in ^{18}O-enriched water led exclusively to the formation of AMP,$^{18}O_1$, identified by ^{31}P NMR, and ADP, proving that enzyme-mediated hydrolysis occurs only at P_α and P'_α of the substrate and not at P_β. Thus, Fhit is an asymmetrical diadenosyl triphosphate hydrolase as is the diadenosyl triphosphate hydrolase found in yellow lupine seeds (*30*).

Table 1: ^{31}P NMR Parameters for Compounds Synthesized

compound	$\delta_{P\alpha}$ (ppm)	$\delta_{P\beta}$ (ppm)	$\delta_{P\gamma}$ (ppm)	^{18}O isotope shift (ppm)
AMP	2.600	–	–	–
AMP,$^{18}O_1$	2.562	–	–	0.038
ADP	−9.2	−4.5	–	–
*m*NBD	−11.0	−4.75	–	–
AMPS	44.25	–	–	–
AMPS,$^{18}O_1$	44.212	–	–	0.038
*m*NBATP	−10.5	−23.0	−11.1	
(S_P)-*m*NBATPαS	44.45	−22.721 −23.053	−10.28	–
(R_P)-*m*NBATPαS	44.15	−22.964 −23.266	−10.55	–
(S_P)-ATPαS	44.301	−22.301	−4.47	
(S_P)-ATPαS,$^{18}O_1$[a]	44.276	−22.319	−4.47	0.024 (P_α) and 0.018 (P_β)
(S_P)-ATPαS,$^{18}O_1$[b]	44.263	−22.301	−4.47	0.038

[a] From AMPαS,$^{18}O_1$ obtained as the Fhit-catalyzed hydrolysis product of (S_P)-*m*NBATPαS in $H_2{}^{18}O$ (40% enrichment) after enzymatic phosphorylation (AK/PK). [b] From AMPαS,$^{18}O_1$ obtained as the Fhit-catalyzed hydrolysis product of (R_P)-*m*NBATPαS in $H_2{}^{18}O$ (50% enrichment) after enzymatic phosphorylation (AK/PK).

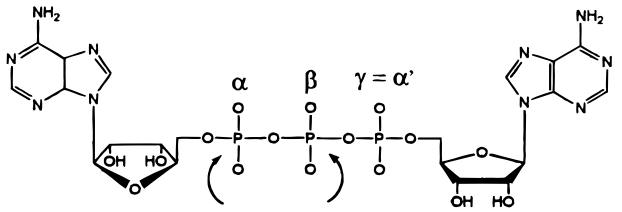

Diadenosine triphosphate

FIGURE 1: Orientation of cleavage in Fhit-catalyzed hydrolysis of Ap_3A. Water or hydroxide may in principle hydrolyze diadenosyl triphosphate at the α-, α′ (=γ)-, or β-phosphorus to produce the products AMP and ADP. Fhit-catalyzed hydrolysis of Ap_3P in ^{18}O-enriched water exclusively produces AMP,$^{18}O_1$, demonstrating that the cleavage occurs at the α- or α′-phosphorus.

Table 2: Kinetic Parameters for Fhit-Catalyzed Hydrolysis of Nucleotides

nucleotide	V_{max} ($\times 10^{-6}$ mol min^{-1} mg^{-1})	K_M (μM)	V^{rel}	products
AP_3A[a,b]	105	1	1	AMP, ADP (1:1)
*m*NBATP[b]	90.3	6.5 ± 1	0.86	AMP, *m*NBDP (1:1)
(S_P)-*m*NBATPαS	0.35	2.8 ± 0.22	0.0033	AMPS, *m*NBDP (1:1)
(R_P)-*m*NBATPαS	0.57	4.6 ± 0.4	0.0054	AMPS, *m*NBDP (1:1)
Ap_3G	–	–	0.44	AMP, GDP (1:1) GMP, ADP (0.2:0.2)

[a] Data for Ap_3A and Ap_3G are from refs *8* and *17*. [b] Data were confirmed for Ap_3A and *m*NBATP by UV/vis analysis.

m-Nitrobenzyl Esters of ATP as Substrates for Fhit. *m*NBATP was evaluated as a substrate for the enzyme by analysis of the reaction products by analytical anion-exchange chromatography. This compound was cleaved only at the nucleotide moiety by the enzyme, and both epimeric phosphorothioates bearing stereochemical information at P_α were also cleaved exclusively at the labeled phosphorus atom (Table 2), although reacting much more slowly. The K_m values for reactions of *m*NBATP, (S_P)-*m*NBATPαS, and (R_P)-*m*NBATPαS were determined by analytical HPLC (Table 2). Compared with the K_m for reaction of Ap_3A, these substrate analogues are bound to the enzyme almost as well as Ap_3A. Moreover, the V_{max} value for reaction of *m*NBATP

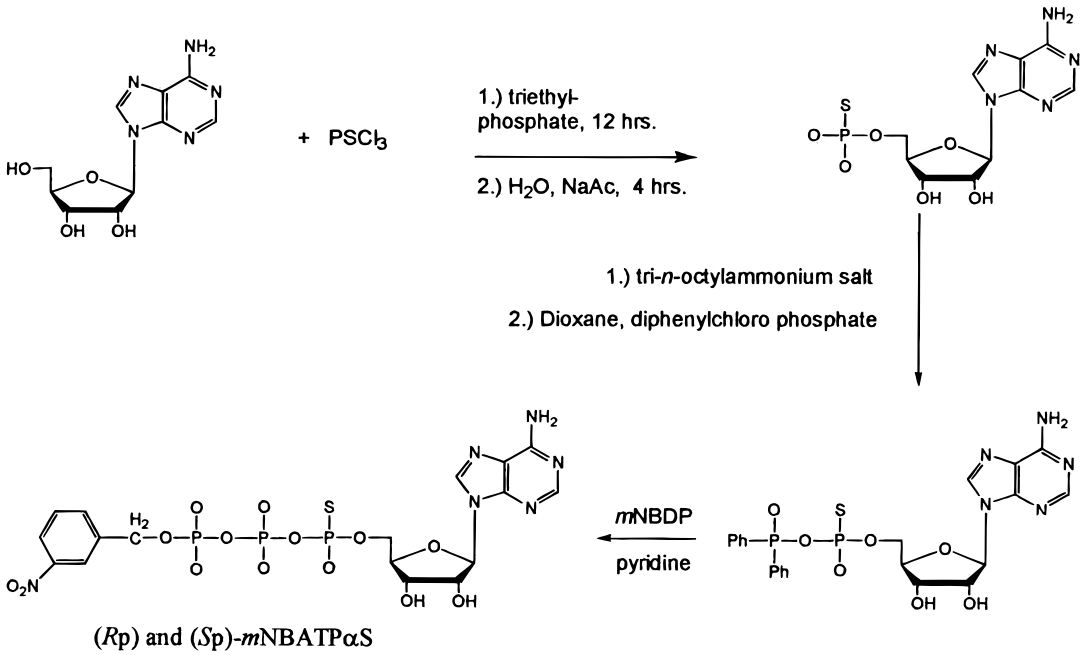

FIGURE 2: Synthesis of (R_P)- and (S_P)-*m*NBATPαS. AMPS is synthesized from adenosine and $PSCl_3$ in $POEt_3$ and activated with diphenylphosphorochloridate in dioxane (*29*). *m*NBDP is coupled to the activated AMPS in pyridine to yield a mixture of two phosphate epimers, which are well-separated by reversed phase HPLC.

is comparable to that for Ap_3A. This indicates that only one nucleotide moiety of the substrate has to be bound by the enzyme in the active site where hydrolysis takes place.

The simplest interpretation of these observations is that the nature of the second esterifying alkyl group at P_γ is largely kinetically irrelevant (*8*, *16*). This is also consistent with the fact that asymmetric dinucleoside triphospates such as Gp_3A are cleaved. Weaker interactions of guanosine in the active site (compared to those of adenosine) lead to slower hydrolysis of this substrate at the guanosine site and the formation of more GDP than ADP. With *m*NBATP as a substrate, hydrolysis occurs only when the molecule is bound to the enzyme with the adenosine moiety accessible to the catalytically relevant histidines. No ADP, the product of hydrolysis at P_γ, is detected by analytical HPLC. The crystal structure of the Fhit−AMP complex (*16*) depicts a complex network of hydrogen bonds from the enzyme to the bound nucleoside and the phosphate. Such hydrogen bonds are still possible when adenine is substituted with guanine but not to the *m*-nitrobenzyl group. The proposed absence of binding to the *m*-nitrobenzyl group is also consistent with the slow reactivity of ATP, less than $^1/_{300}$th of the rate of Ap_3A, as a substrate. Under the reaction conditions, ATP exists as its Mg^{2+} complex, and MgATP is electrostatically and structurally very different from a P_γ-alkyl ester of ATP, which does not bind Mg^{2+} as tightly as does ATP, and would not exist as Mg^{2+} complexes under the reaction conditions. The role of divalent cations for overall enzyme activity is not clear, but evidently, a cation-complexed substrate is not required by the enzyme (*16*). However, divalent cations might have structural functions on the enzyme.

Thiophosphates are generally slower substrates for their specific enzymes than the corresponding phosphates. When (S_P)-*m*NBATPαS or (R_P)-*m*NBATPαS is used as a substrate for Fhit, the V_{max} is decreased about 200−300-fold. Inasmuch as only AMPS and *m*NBDP are the reaction products, the phosphorus atom next to the *m*-nitrobenzyl group is not the locus of hydrolysis. This confirms that binding of the *m*-nitrobenzyl group by the enzyme is weak and does not allow hydrolysis at P^3 of the molecule. However, the K_m values for reactions of both epimers indicate that the AMPS moiety is bound almost as tightly as AMP in *m*NBATP and Ap_3A.

Synthesis of Phosphorus-Chiral Substrates. The synthesis of (S_P)-*m*NBATPαS and (R_P)-*m*NBATPαS is outlined in Figure 2. Coupling of *m*-nitrobenzyl bromide to pyrophosphate in dry acetonitrile yields *m*NBDP, which is then coupled to activated AMPS by the Michelson anhydride method (*29*). Although *m*NBDP is contaminated with about 20% pyrophosphate which also reacts with the activated AMPS to yield the two epimers of ATPαS, they are removed from the desired molecules by chromatography on a DEAE-Sephadex A-25 column. Pyrophosphate can be completely removed from *m*NBDP by inorganic pyrophosphatase, which does not catalyze hydrolysis of *m*NBDP (data not shown). The ratio of (S_P)-*m*NBATPαS to (R_P)-*m*NBATPαS was consistently found to be 1:3 throughout all our preparations, and baseline separation of both epimers was achieved by HPLC on a reversed phase column under isocratic conditions in 10 mM potassium phosphate and 7.5% MeOH. Inorganic phosphate was removed from the purified epimers by rechromatography on a short DEAE-Sephadex A-25 column. ^{31}P NMR of the compounds (see Table 1) as well as analytical HPLC on a reversed phase column proved the purity of both individual compounds and allowed the assignment of the configurations at P_α.

Stereochemical Course of Fhit-Catalyzed Hydrolysis. Hydrolysis of the individual phosphate epimers of *m*NBATPαS in ^{18}O-enriched water was performed in the presence of 1200 units of Fhit. The enzyme was stored in 10% glycerol, which was decreased to <0.5% by dialysis. The level of ^{18}O enrichment of the water used in the experiment was 50% in the experiment with (R_P)-*m*NBATPαS and 40% in the reaction of (S_P)-*m*NBATPαS. Unlabeled AMPS and (S_P)-

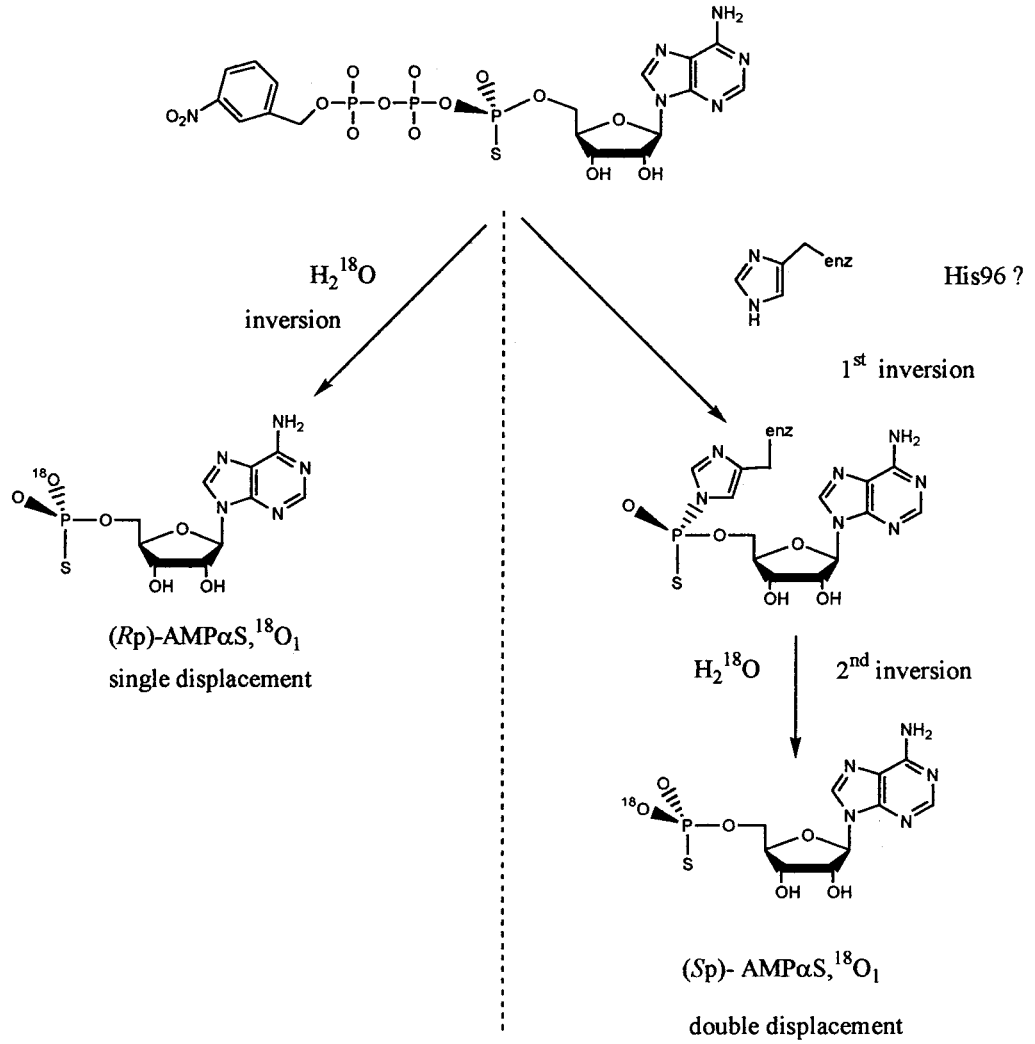

FIGURE 3: Two possible mechanisms for the hydrolysis of (R_P)-*m*NBATPαS by Fhit in $H_2{}^{18}O$. The consequence of a direct nucleophilic attack of ^{18}O-enriched water on the stereochemical configuration at the α-phosphorus atom of the substrate analogue is shown on the left. Here, a single-displacement mechanism with inversion of configuration leads to formation of (R_P)-AMPS,$^{18}O_1$. On the right, a nucleophilic attack of a nitrogen atom of a histidine in the active site of the protein leads to inversion of configuration at the phosphorus atom, and the resulting adenylylated enzyme intermediate is shown. In a second nucleophilic attack on the phosphorus atom of the nucleotidylated enzyme by ^{18}O-enriched water, the configuration at phosphorus is inverted back to its original configuration. The result of this double-displacement mechanism is overall retention of configuration, and the product is (S_P)-AMPS,$^{18}O_1$. The structure of the AMP−enzyme intermediate linked through a histidine residue is illustrative and not intended to specify which nitrogen of the histidine side chain is bonded to the AMP moiety. The regiochemistry of His96 is shown in Figure 7.

ATPαS served as internal standards for assigning the chemical isotope shifts in the ^{31}P NMR experiments.

The two possible mechanisms for the enzyme-catalyzed hydrolysis of these substrates, double displacement versus single displacement, are outlined in Figure 3. The hydrolysis of the epimers was performed at 27 °C, and careful adjustment of the pH to 8 had to be carried out to avoid loss of the acid labile sulfur on AMPS because hydrolysis is accompanied by the release of a proton that lowers the pH. The reaction reached completion within 3 h, and approximately 15% of the AMP resulting from desufurization of AMPS was removed on the anion-exchange column.

The two phosphate-bound oxygen atoms in unlabeled AMPS are diastereotopic, and replacement of one oxygen atom by a heavy isotope leads to the formation of phosphate-chiral AMPS. The stereochemistry of the phosphorylation of AMPS by adenylate kinase (*31*) and pyruvate kinase in the presence of phosphoenolpyruvate and catalytic amounts of ATP has been explored by Sheu et al. (*32*). Adenylate kinase phosphorylates AMPS with high stereoselectivity to produce (S_P)-ADPαS, which is further phosphorylated to (S_P)-ATPαS by pyruvate kinase. The high degree of stereoselectivity makes this enzymatic system a powerful tool for exploiting the stereochemistry of enzyme reactions leading to the formation of chiral AMPS. When (S_P)-*m*NBATPαS or (R_P)-*m*NBATPαS is hydrolyzed by Fhit in ^{18}O-enriched water to AMPS,$^{18}O_1$, phosphate-chiral AMPS is produced. Phosphorylation of the individual chiral compounds to (S_P)-ATPαS,$^{18}O_1$ by the adenylate kinase/pyruvate kinase system (Figure 4) and subsequent ^{31}P NMR analysis of the compounds revealed the stereochemistry of hydrolysis at the α-phosphorus atom of the substrate and ultimately documented the mechanism by which hydrolysis is carried out by the enzyme. If, for example, (S_P)-*m*NBATPαS is attacked on P_α by $H_2{}^{18}O$ according to a single-displacement mechanism, inversion of configuration at the phosphorus atom would occur, thus leading to formation of (S_P)-AMPS,$^{18}O_1$. A double-displacement mechanism, with His96 covalently

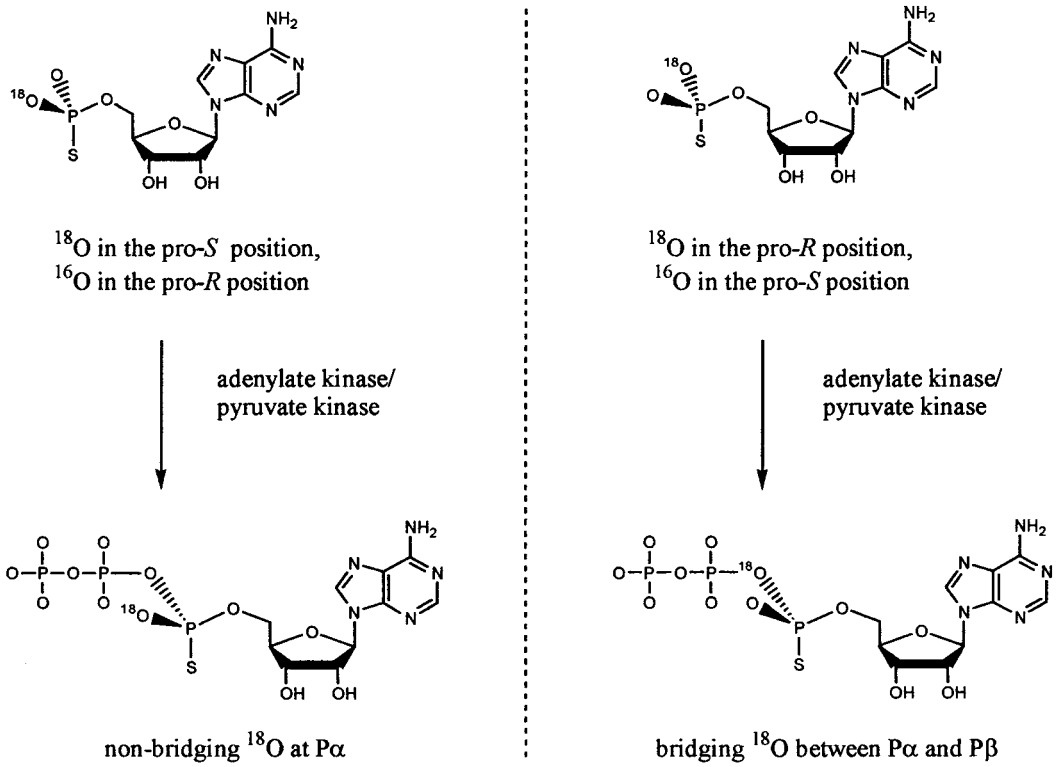

FIGURE 4: Stereospecific phosphorylation of phosphate-chiral AMPS,$^{18}O_1$. Adenylate kinase catalyzes the phosphorylation of AMPS to (S_P)-ADPαS, and pyruvate kinase catalyzes its further phosphorylation to (S_P)-ATPαS. When ^{18}O is in the S_P position, as on the left, it is not phosphorylated and ^{18}O is nonbridging in the product. When ^{18}O is in the R_P position, as on the right, it is phosphorylated and ^{18}O is found in the bridging position of the product.

bonded to AMPS as an intermediate that is subsequently hydrolyzed by $H_2{}^{18}O$, results in retention of the configuration at P_α, thus yielding (R_P)-AMPS,$^{18}O_1$. Similarly, (R_P)-*m*NBATPαS gives rise to (S_P)-AMPS,$^{18}O_1$ by a double-displacement and (R_P)-AMPS,$^{18}O_1$ by a single-displacement mechanism (Figure 3).

AMPS,$^{18}O_1$ from the hydrolysis of (S_P)-*m*NBATPαS in 40% ^{18}O-enriched water was phosphorylated by the adenylate kinase/pyruvate kinase system to produce (S_P)-ATPαS,$^{18}O_1$, with ^{18}O bridging P_α and P_β. The chemical shifts of P_α and P_β in unlabeled (S_P)-ATPαS were 44.301 and −22.201 ppm, respectively. The isotope shifts in the ^{31}P NMR due to bridging ^{18}O in the compound were 0.023 ppm in the low-field doublet signal (P_α centered at 44.324 ppm) and 0.020 ppm in the high-field doublet doublet centered at −22.224 ppm (Figure 6). This meant that Fhit catalyzed the hydrolysis of (S_P)-*m*NBATPαS to (R_P)-AMPS,$^{18}O_1$ via a double-displacement mechanism. This result was confirmed by the analysis of the AMPS,$^{18}O_1$ obtained from catalytic hydrolysis of (R_P)-*m*NBATPαS in 50% ^{18}O-enriched water. The low-field signal of P_α of (S_P)-ATPαS,$^{18}O_1$ was now centered at 44.338 ppm. The magnitude of the ^{18}O isotope shift was 0.037 ppm, and no isotope shift was detected at the high-field doublet doublet signal of P_β at −22.201 ppm (Figure 5). The magnitude of the isotope shifts at P_α of 0.037 ppm, compared with 0.023 ppm for singly bonded ^{18}O, is indicative of nonbridging ^{18}O. Therefore, (R_P)-*m*NBATPαS must have been hydrolyzed to (R_P)-AMPS,$^{18}O_1$ in the same way as (S_P)-*m*NBATPαS was hydrolyzed to (S_P)-AMPS,$^{18}O_1$, that is, with overall retention of the configuration at phosphorus.

The mechanism proposed for the action of Fhit in the reaction of (R_P)-*m*NBATPαS is shown in Figure 7 and is

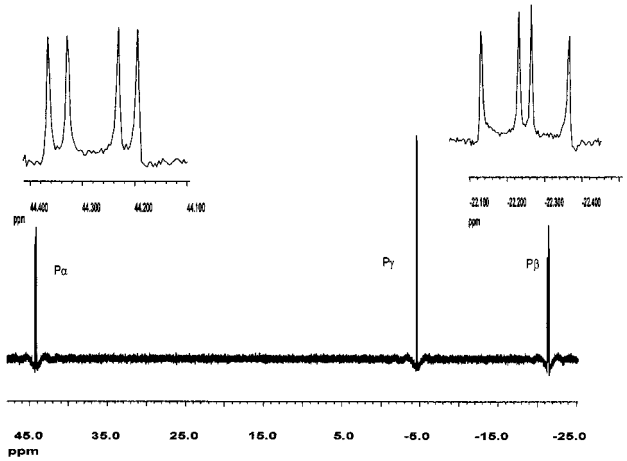

FIGURE 5: ^{31}P NMR spectrum in the P_α and P_β regions of (S_P)-ATPαS derived from hydrolysis of (R_P)-mNBATPαS in 50% ^{18}O-enriched $H_2{}^{18}O$. The P_α signal is in the low-field range of the spectrum at 44.301 ppm. Next to this doublet centered at 44.263 ppm is the signal of the labeled (S_P)-ATPαS,$^{18}O_1$. The isotope shift of the P_α signal is 0.038 ppm, corresponding to nonbridging ^{18}O, and no isotope-shifted feature is present in the P_β signal, which is centered at −22.301 ppm (two doublets). This result proved that (R_P)-*m*NBATPαS was hydrolyzed by Fhit to (S_P)-AMPαS,^{18}O with overall retention of configuration at P_α.

based on the results presented here as well as the crystal structure of the complex of Fhit with AMP (*16*). The mechanism is analogous to that demonstrated for *E. coli* GalT (*18*, *23*). The interactions of the three histidine residues with the substrate in Figure 7 are as follows. The $N^{\delta 1}H$ atom of His96 forms a hydrogen bond to the main chain carbonyl group of His94 and thereby activates $N^{\epsilon 2}$ of His96 for nucleophilic attack on P_α of the substrate. His96 is placed

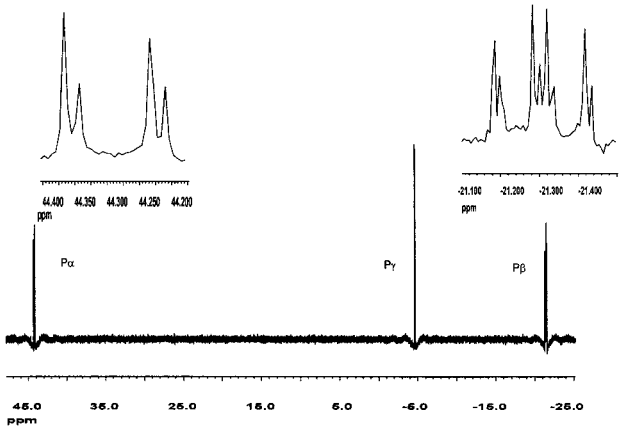

FIGURE 6: ^{31}P NMR spectrum in the P_α and P_β regions of (S_P)-ATPαS,$^{18}O_1$ derived from hydrolysis of (S_P)-mNBATPαS in 40% ^{18}O-enriched $H_2{}^{18}O$. The P_α signal of unlabeled (S_P)-ATPαS is in the low-field range of the spectrum at 44.301 ppm. Next to this doublet centered at 44.276 is the signal of the labeled (S_P)-ATPαS,$^{18}O_1$. The isotope shift of the P_α signal is 0.024 ppm, corresponding to a bridging ^{18}O between P_α and P_β. Centered at −22.301 ppm are the two doublets belonging to P_β of the unlabeled (S_P)-ATPαS, and at −22.319 ppm, shifted by 0.018 ppm, are the two doublets of labeled (S_P)-ATPαS,$^{18}O_1$. This result showed that (S_P)-*m*NBATPαS was hydrolyzed by Fhit in ^{18}O-enriched water to (R_P)-AMPS,$^{18}O_1$ with overall retention of configuration at P_α.

rather rigidly in the active site and is in position to attack P_α. The role of His98 is not clear; however, an apparent hydrogen bond to one of the oxygen atoms of P_α would be analogous to the interaction of the corresponding Gln168 in GalT and could position the substrate for access to His96. Upon adenylylation of His96 with inversion of configuration at P_α, the hydrogen bond between the main chain carbonyl of His94 and $N^{\delta1}H$ of His96 presumably immobilizes the proton and maintains the adenylyl group in a reactive state. Deadenylylation by water produces AMPS,^{18}O with a second inversion of configuration, accounting for overall retention of configuration at P_α. The mechanism of nucleotidyl transfer by GalT from *E. coli* is similar, with His164, His166, and Gln168 carrying out the functions of His94, His96, and His98 in Figure 7.

Studies on possible intermediates, the stereochemical course of the reaction, and substrate analogues have not been carried out with the Fhit homologue, *S. pombe* Ap_4A hydrolase. Studies on Ap_4A asymmetric hydrolases from *Artemia* and yellow lupin indicate that these enzymes facilitate H_2O attack at the fourth P from a nucleoside in Np_nN', where $n = 4-6$ (NTP is always a product). This was determined from substrate and product specificity and use of $H_2{}^{18}O$ as a substrate followed by mass spectrometry (*30*, *33*, *34*). P^1 and P^4 chiral isomers of Ap_4A containing different isotopic forms of O have been used to show that the lupin Ap_4A hydrolase reaction proceeds with inversion of configuration at the attacked P (*35*). Thus, these enzymes probably work via a single-displacement mechanism with no covalent intermediate. Lupin Ap_4A hydrolase is not a member of the GAFH superfamily, but is considered a member of the nudix family of proteins (*36*) because of the presence of a MutT sequence motif (*37*). Ap_4A phosphorylase I has been shown to retain the substrate P_α configuration, phosphorolyzing (S_P)-$Ap_4A\alpha S$ to (S_P)-ADPαS (*38*, *39*). This implies that the enzyme forms a covalent AMP−enzyme intermediate. Booth and Guidotti (*40*) showed that a putative polyphosphate

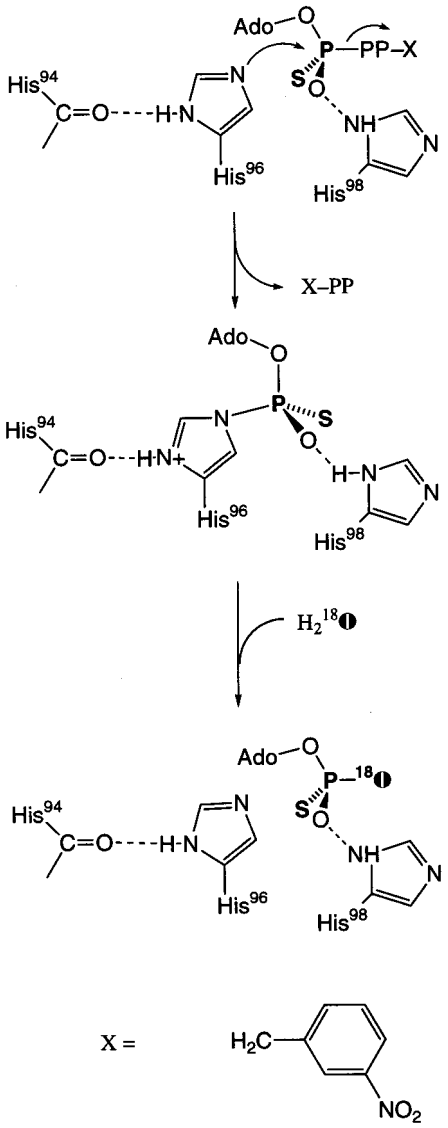

FIGURE 7: Mechanism of hydrolysis of (R_P)-*m*NBATPαS by Fhit in ^{18}O-enriched water. On the basis of the crystal structure of Fhit in complex with AMP (*16*), His96 is coordinated through its $N^{\delta1}H$ to the main chain carbonyl group of His94. Catalysis proceeds through nucleophilic attack of the $N^{\epsilon2}$ atom of His96 on P_α of the substrate analogue, leading to inversion of configuration at phosphorus and release of *m*NBDP. Nucleophilic attack of the ^{18}O atom of water in the hydrolytic step inverts the configuration at P_α of the adenylylated enzyme intermediate, and the bond to the histidine is broken. The configuration at P_α of the product is the same as in the initial substrate. Throughout catalysis, His98 remains coordinated to a peripheral oxygen atom at P_α of the substrate analogue.

kinase in yeast was actually the Ap_4A phosphorylase and presented data for an AMP−enzyme intermediate. Ap_4A phosphorylase I can catalyze an exchange reaction between the β-phosphate of nucleoside diphosphates (NDP) and P_i that is faster than the Ap_4A cleavage (*41*). This is an exchange reaction expected for a ping-pong mechanism. Thus, three different enzymes, Fhit, GalT, and Ap_4A phosphorylase I, each representative of one protein subfamily of the GAFH superfamily, exhibit the same stereochemistry of reaction of their respective substrate with overall retention of configuration of the α-phosphorus. A mechanistic similarity is now included along with sequence and structural similarities among these enzymes.

Nonstereoselectivity of Fhit for Phosphate Epimers of mNBATPαS. Enzymes that catalyze substitution at P_α of nucleoside polyphosphates generally display a strong preference for one epimer of the corresponding P_α-thio substrates (*42*, *43*). DNA and RNA polymerases preferentially accept the S_P epimers of dATPαS and ATPαS, respectively. Galactose-1-phosphate uridylyltransferase preferentially accepts the R_P epimers of UDPαS-glucose and UDPαS-galactose. The absence of significant stereoselectivity in the interactions of Fhit with the phosphate epimers of *m*NBATPαS is unusual and further supports the idea that binding to the alkyl group bonded to P_γ may not be important. An absence of binding to the P_γ-alkyl group could lend structural flexibility to the polyphosphate and allow either α-phosphate epimer of *m*NBATPαS to adopt a reactive conformation.

ACKNOWLEDGMENT

We thank Dr. Kay Huebner for originally providing the *FHIT* cDNA. We thank Barbara Garratana for providing an initial test sample of *m*NBATP.

REFERENCES

1. Ohta, M., Inoue, H., Cotticelli, M. G., Kastury, K., Baffa, R., Palazzo, J., Siprashvili, Z., Mori, M., McCue, P., Druck, T., Croce, C. M., and Huebner, K. (1996) *Cell 84*, 587−597.
2. Huebner, K., Hadaczek, P., Siprashvili, Z., Druck, T., and Croce, C. M. (1997) *Biochim. Biophys. Acta 1332*, M65−M70.
3. Sozzi, G., Huebner, K., and Croce, C. M. (1998) *Adv. Cancer Res. 74*, 141−166.
4. LeBeau, M. M., Drabkin, H., Glover, T. W., Gemmill, R., Rassool, F. V., McKeithan, T. W., and Smith, D. 1. (1998) *Genes, Chromosomes Cancer 21*, 281−289.
5. Huebner, K., Garrison, P. N., Barnes, L. D., and Croce, C. M. (1998) *Annu. Rev. Genet. 32*, 7−31.
6. Siprashvili, Z., Sozzi, G., Barnes, L. D., McCue, P., Robinson, A. K., Eryomin, V., Sard, L., Tagliabue, E., Greco, A., Fusetti, L., Schwartz, G., Pierotti, M. A., Croce, C. M., and Huebner, K. (1997) *Proc. Natl. Acad. Sci. U.S.A. 94*, 13771−13776.
7. Huang, Y., Garrison, P. N., and Barnes, L. D. (1995) *Biochem. J. 312*, 925−932.
8. Barnes, L. D., Garrison, P. N., Siprashvili, Z., Guranowski, A., Robinson, A. K., Ingram, S. W., Croce, C. M., Ohta, M., and Huebner, K. (1996) *Biochemistry 35*, 11529−11535.
9. Chen, J., Brevet, A., Blanquet, S., and Plateau, P. (1998) *J. Bacteriol. 180*, 2345−2349.
10. Séraphin, B. (1992) *DNA Sequence 3*, 177−179.
11. Brenner, C., Garrison, P. N., Gilmour, J., Peisach, D., Ringe, D., Petsko, G. A., and Lowenstein, J. M. (1997) *Nat. Struct. Biol. 4*, 231−238.
12. Field, T. L., Reznikoff, W. S., and Frey, P. A. (1989) *Biochemistry 28*, 2094−2099.
13. Wedekind, J. E., Frey, P. A., and Rayment, I. (1995) *Biochemistry 34*, 11049−11061.
14. Lima, C. D., Klein, M. G., Weinstein, 1. B., and Hendrickson, W. A. (1996) *Proc. Natl. Acad. Sci. U.S.A. 93*, 5357−5362.
15. Holm, L., and Sander, C. (1997) *Trends Biochem. Sci. 22*, 116−117.
16. Lima, C. D., D'Amico, K. L., Naday, I., Rosenbaum, G., Westbrook, E. M., and Hendrickson, W. A. (1997) *Structure 5*, 763−774.
17. Pace, H. C., Garrison, P. N., Robinson, A. K., Barnes, L. D., Draganescu, A., Rösler, A., Blackburn, G. M., Siprashvili, Z., Croce, C. M., Huebner, K., and Brenner, C. (1998) *Proc. Natl. Acad. Sci. U.S.A. 95*, 5484−5489.
18. Frey, P. A., Wong, L. J., Sheu, K.-F. R., and Yang, S. L. (1982) *Methods Enzymol. 87*, 20−36.
19. Wong, L. J., Sheu, K.-F. R., Lee, S. L., and Frey, P. A. (1977) *Biochemistry 16*, 1010−1016.
20. Sheu, K.-F. R., Richard, J. P., and Frey, P. A. (1979) *Biochemistry 18*, 5548−5556.
21. Arabshahi, A., Brody, R. S., Smallwood, A., Tsai, T.-C., and Frey, P. A. (1986) *Biochemistry 25*, 5583−5589.
22. Kim, J., Ruzicka, F., and Frey, P. A. (1990) *Biochemistry 29*, 10590−10593.
23. Wedekind, J. E., Frey, P. A., and Rayment, I. (1996) *Biochemistry 35*, 11560−11569.
24. Lima, C. D., Klein, M. G., and Hendrickson, W. A. (1997) *Science 278*, 286−290.
25. Brenner, C., Pace, H. C., Garrison, P. N., Robinson, A. K., Rösler, A., Liu, X.-H., Blackburn, G. M., Croce, C. M., Huebner, K., and Barnes, L. D. (1997) *Protein Eng. 10*, 1461−1463.
26. Moellering, H., and Bergmeyer, H.-U. (1963) *Methods of enzymatic analysis*, pp 578−580.
27. Davisson, V. J., Davis, D. R., Dixit, V. M., and Poulter, C. D. (1987) *J. Org. Chem. 52*, 1794−1801.
28. Murray, A. W., and Atkinson, M. R. (1968) *Biochemistry 7*, 4023−4029.
29. Michelson, A. M. (1964) *Biochim. Biophys. Acta 91*, 1−13.
30. Guranowski, A., Brown, P., Ashton, P. A., and Blackburn, G. M. (1994) *Biochemistry 33*, 235−240.
31. Eckstein, F., and Goody, R. S. (1976) *Biochemistry 15*, 1685−1691.
32. Sheu, K.-F. R., and Frey, P. A. (1977) *J. Biol. Chem. 252*, 4445−4448.
33. Blackburn, G. M., Taylor, G. E., Thatcher, G. R. J., Prescott, M., and McLennan, A. G. (1987) *Nucleic Acids Res. 15*, 6991−7004.
34. McLennan, A. G., Prescott, M., and Evershed, R. P. (1989) *Biomed. Environ. Mass Spectrosc. 18*, 450−452.
35. Dixon, R. M., and Lowe, G. (1989) *J. Biol. Chem. 264*, 2069−2074.
36. Bessman, M. J., Frick, D. N., and O'Handley, S. F. (1996) *J. Biol. Chem. 271*, 25059−25062.
37. Maksel, D., Guranowski, A., Ilgoutz, S. C., Moir, A., Blackburn, M. G., and Gayler, K. R. (1998) *Biochem. J. 329*, 313−319.
38. Lazewska, D., and Guranowski, A. (1990) *Nucleic Acids Res. 18*, 6083−6088.
39. Blackburn, G. M., Guo, M.-J., and McLennan, A. G. (1992) in *Ap_4A and Other Dinucleoside Polylphosphates* (McLennan, A. G., Ed.) pp 305−342, CRC Press, Boca Raton, FL.
40. Booth, J. W., and Guidotti, G. (1995) *J. Biol. Chem. 270*, 19377−19382.
41. Guranowski, A., and Blanquet, S. (1986) *J. Biol. Chem. 261*, 5943−5946.
42. Frey, P. A. (1992) *Enzymes (3rd ed.) 20*, 141−185.
43. Frey, P. A. (1989) *Adv. Enzymol. Relat. Areas Mol. Biol. 62*, 119−201.

BI981895J